



# Silicon sawing waste treatment by electrophoresis and gravitational settling

Tzu-Hsuan Tsai\*

Department of Materials and Mineral Resources Engineering, National Taipei University of Technology, Taipei 10608, Taiwan

## ARTICLE INFO

### Article history:

Received 16 December 2010  
Received in revised form 20 February 2011  
Accepted 21 February 2011  
Available online 26 February 2011

### Keywords:

Electrophoresis  
Gravitational settling  
Silicon  
Silicon carbide  
Alumina  
Recovery

## ABSTRACT

In silicon wafer manufacturing for solar cells, a great amount of hazardous sawing waste with tiny Si particles is produced, resulting in serious environmental problems. Recycling Si and abrasives from the waste is regarded as an effective solution. Based on the view of recycling,  $\text{Al}_2\text{O}_3$  might be good abrasives for cutting Si ingot due to its larger density and higher isoelectric point than SiC. This study reports the separation of Si/SiC and Si/ $\text{Al}_2\text{O}_3$  mixtures by electrophoresis and gravitational settling. At pH 9, nearly uncharged  $\text{Al}_2\text{O}_3$  settled quickly and the negatively charged Si moved toward the anode, leading to an obvious Si distribution on the cell bottom. The experimental results show the separation performance of Si and  $\text{Al}_2\text{O}_3$  at pH 9 was better than at pH 2.5, and the performance was higher than that between Si and SiC. The minimum and maximum  $\text{Al}_2\text{O}_3$  contents remaining in Si/ $\text{Al}_2\text{O}_3$  mixture were 9 wt% and 90 wt% after applying 1 V/cm for 24 h at pH 9. The recovered material with high Si content can be considered as a new Si source for solar cell, and the abrasives can be reused in the sawing process.

© 2011 Elsevier B.V. All rights reserved.

## 1. Introduction

In Si wafer manufacturing, there is a kerf loss of over 50% for every Si ingot during the sawing process [1]. This kerf Si drains away with the slurry waste, which contains abrasives, lubricating liquid and steel residue from the sawing wires. A great amount of sawing waste is treated by incineration equipment or by a wastewater treatment facility, resulting in the generation of carbon dioxide or sludge. From an environmental point of view, these disposal methods are unfavorable, and the tiny particles, around 0.1–100  $\mu\text{m}$ , in the sawing waste are hazardous for health. In fact, the Si kerf and abrasives in the waste are still usable. Recovering Si from sawing slurry waste is regarded as an effective solution for overcoming silicon feedstock shortages [1,2], and recycling abrasives can decrease the operation cost and reduce the amount of waste product [3].

The main challenge in recycling sawing waste is the separation of Si and abrasives, Si and SiC especially [4]. Several studies with regard to separation of Si or SiC have been done. Mühlbauer et al. [5] utilized a directional solidification process to remove C and SiC from Si materials produced via silica reduction in an arc furnace. Nishijima et al. [6] applied superconducting magnetic methods to acquire SiC from sawing waste. Shibata et al. [7] used flotation to obtain SiC from sawing wastes. Zhang and Ciftja [8] investigated the removal of SiC and  $\text{Si}_3\text{N}_4$  inclusions from top-cut solar cell Si scraps by filtration with foam filters. Wang et al. [9,10] and

Lin et al. [11] developed a process for purifying the Si obtained from slurry. Their method includes chemical treatment, heavy-fluid high-gravity centrifugation, high-temperature treatment, and directional solidification. Their studies emphasize the importance of Si preconcentration before high-temperature steps although SiC particles could not be removed completely from the mixture [9].

Moreover, because SiC particles in sawing waste have greater density, surface charges, and particle sizes than Si particles, Si and SiC can be separated by electrophoresis and gravitational settling [12]. Based on the view of recycling, the abrasives owning the different properties from Si might be helpful for the separation of Si and abrasives. Alumina ( $\alpha\text{-Al}_2\text{O}_3$ ) owns the greater density and isoelectric point than SiC, and its Mohs scale is 9.0, which is close to the hardness of SiC (9.3) [13]. Therefore,  $\text{Al}_2\text{O}_3$  might be a good candidate for sawing abrasives from the view of recovering slurry wastes. This study explored the separation of Si/SiC and Si/ $\text{Al}_2\text{O}_3$  mixtures by electrophoresis and gravitational settling at the isoelectric point of Si or abrasives. The separation performance of Si/SiC or Si/ $\text{Al}_2\text{O}_3$  was investigated, and the recovered concentration was analyzed.

## 2. Experimental

To fix the composition of samples, solid powders of 30 wt.% Si and 70 wt.% abrasives (SiC or  $\text{Al}_2\text{O}_3$ ) were mixed. The abrasives were purchased from Extec, and both were in the diameter of 10–15  $\mu\text{m}$ . The Si powder was purchased from Strem Chemicals, and the average size is around 10  $\mu\text{m}$ . Before mixing, the Si was fed to a ball mill for 40 min to obtain the particles with the average diameter of 1  $\mu\text{m}$ .

\* Tel.: +886 2 2771 2171x2775; fax: +886 2 2778 7579.  
E-mail address: [tzhtsai@ntut.edu.tw](mailto:tzhtsai@ntut.edu.tw)

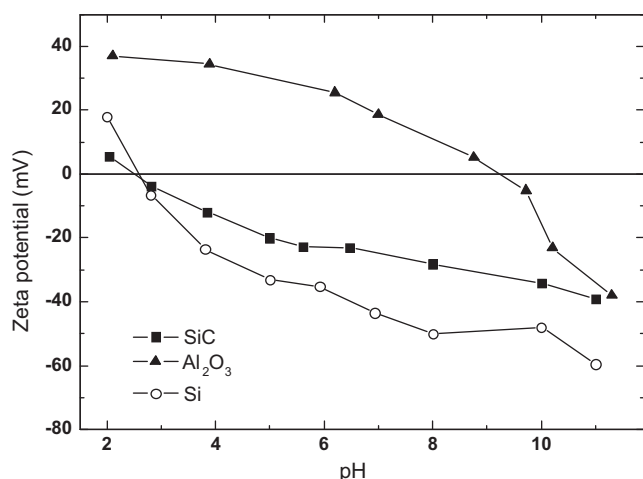


Fig. 1. Zeta potentials of Si, SiC and  $\text{Al}_2\text{O}_3$  in the solutions of different pHs.

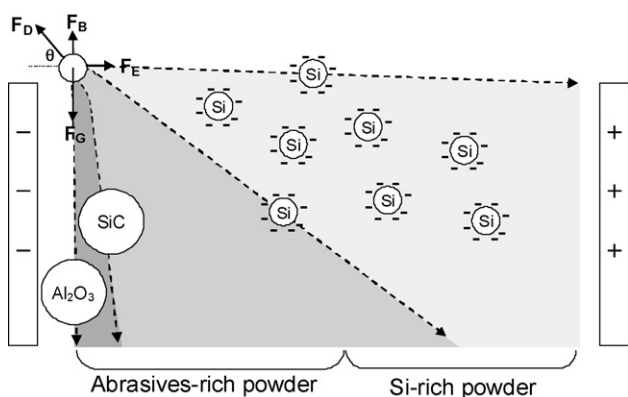


Fig. 2. Schematic diagram of particles moving in an electrical field.

Several properties of the solid mixtures were analyzed. First, the particle size distribution (PSD) was measured using static light scattering (Beckman, Coulter LS230). The carbon content in Si/SiC mixture was verified using a Horiba carbon/sulfur analyzer (model CS-244; Leco). The SiC content was then calculated, and the Si content in the powders was estimated. In addition,  $\text{Al}_2\text{O}_3$  content in Si/ $\text{Al}_2\text{O}_3$  was verified using X-ray fluorescence spectrometer (model RIX2000; Rigaku). A zeta potential analyzer (Zetasizer 3000; Malvern) was used to determine the surface charges on the Si, SiC and  $\text{Al}_2\text{O}_3$  particles at various pHs. The solutions at different pHs were prepared using phosphoric acid and sodium hydroxide.

Solid samples comprised of 15 g Si/abrasives were mixed with 5000 ml of buffer solution and transferred to the separation cell. Buffer solutions with pHs of 2.5 and 9 were prepared using phosphoric acid and sodium hydroxide. The separation cell, with a depth of 15 cm and a length of 15 cm, was designed to separate different particles by electrophoresis and gravitational settling. A power supply and pair of platinized titanium electrodes were used to apply a constant electrical field across the solution in the cell. The details about the separation system were reported previously [12]. In this study, the applied electrical field was 1 V/cm. At the cell bottom, 10 regions were equally divided to collect the settling particles. After operation for 24 h, the specimens collected at different positions were dried and analyzed using static light scattering (Beckman, Coulter LS230) and a Horiba carbon/sulfur analyzer (model CS-244; Leco). The PSD and SiC content at each position were then determined to determine separation performance.

**Table 1**  
Parameters of Si, SiC and  $\text{Al}_2\text{O}_3$  particles at pH=9.

Parameters	Si	SiC	$\text{Al}_2\text{O}_3$
Density ( $\rho$ , g/cm <sup>3</sup> )	2.33	3.16	3.97
Hardness (Mohs scale)	7.0	9.3	9.0
Main diameter ( $d_m$ , $\mu\text{m}$ )	1.0	10	10
Zeta potential ( $\zeta$ , mV)	-48.8	-31.3	1.37
Horizontal displacement ( $d$ , cm)	21	0.12	$1.6 \times 10^{-3}$
Inclined angle ( $\theta$ , degrees)	34.34	89.55	89.99
Time requirement ( $t$ , h)	14	0.089	0.064

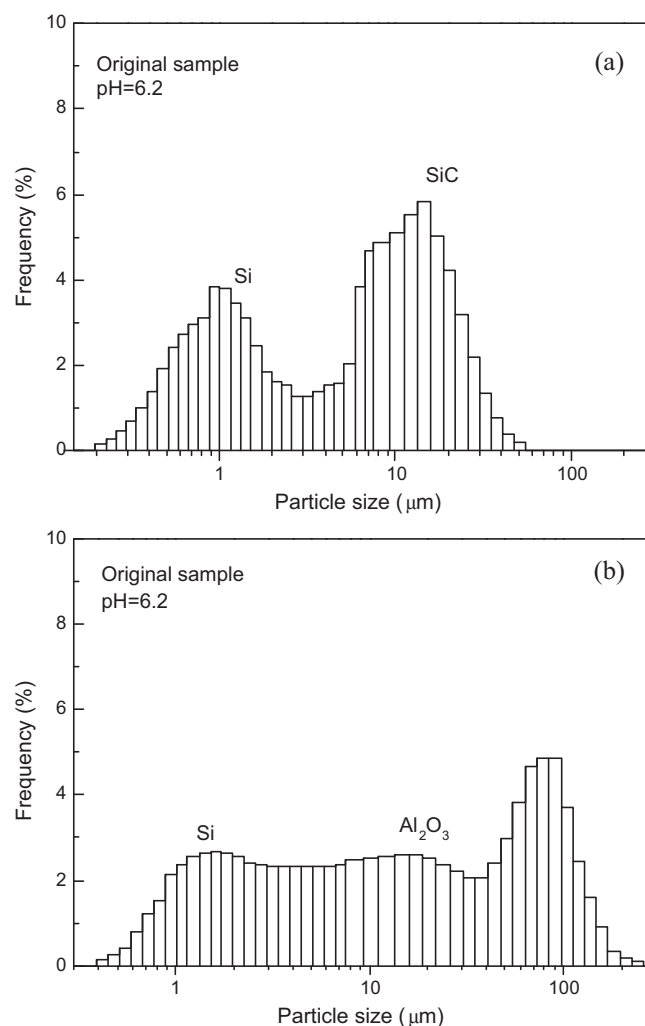
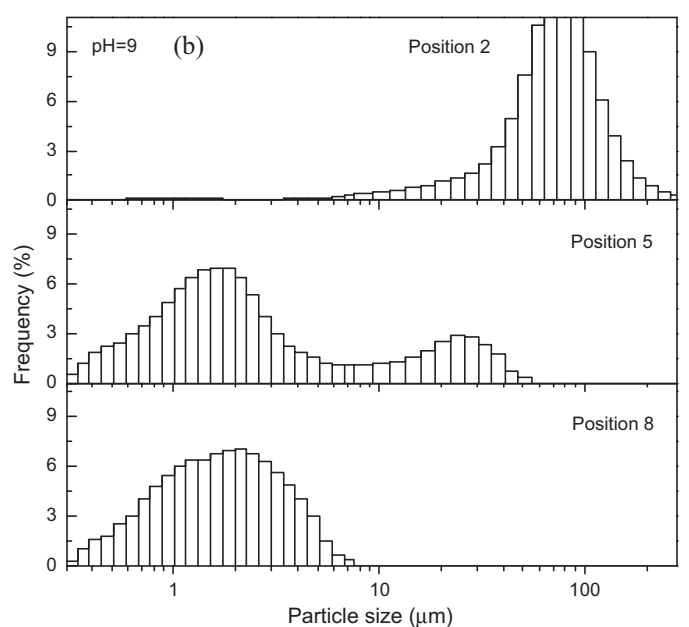
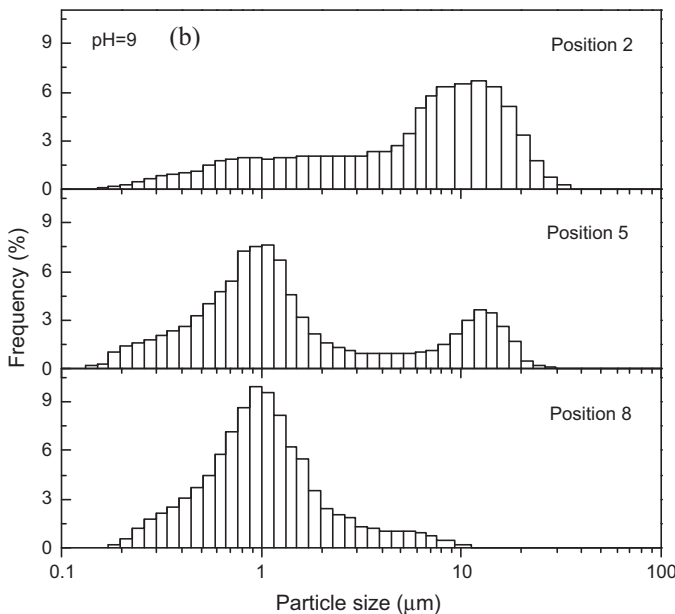
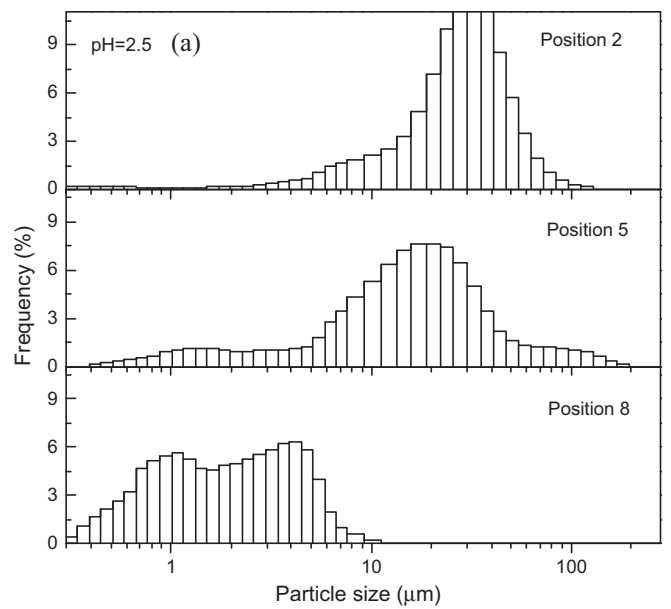
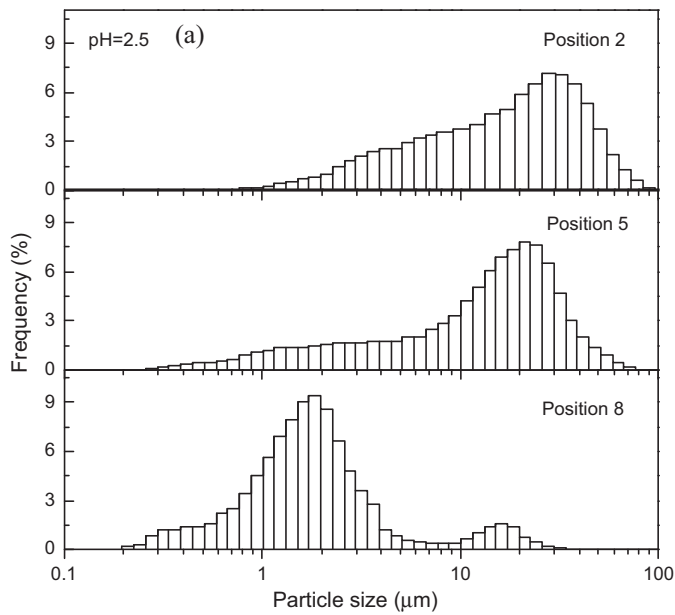


Fig. 3. Particle size distribution of original mixtures. (a) Si/SiC; (b) Si/ $\text{Al}_2\text{O}_3$ .

### 3. Results and discussion

Fig. 1 shows measured results for the zeta potentials of Si, SiC and  $\text{Al}_2\text{O}_3$ . The isoelectric points of Si and SiC were both at pH 2.5, indicating that the surfaces of Si and SiC were positively charged at  $\text{pH} < 2.5$ , and negatively charged at  $\text{pH} > 2.5$ . Therefore, to separate Si from Si/SiC mixture, an applied electrical field induced the same migration direction for Si and SiC. However, the isoelectric point of  $\text{Al}_2\text{O}_3$  was at pH 9, much higher than Si. To separate Si from Si/ $\text{Al}_2\text{O}_3$  mixture in an applied electrical field, the pH of the solution could be set at the isoelectric point of Si or at that of  $\text{Al}_2\text{O}_3$ . Thus, neutrally charged particles would settle directly, while the charged particles would migrate along an applied electrical field. For example, when the solution was controlled at  $\text{pH} = 9$ , the zeta potentials of Si, SiC and  $\text{Al}_2\text{O}_3$  were  $-48.8$  mV,  $-31.3$  mV and  $1.37$  mV, respectively.



**Fig. 4.** Particle size distribution for Si/SiC mixture after separation process. (a) pH=2.5; (b) pH=9.

**Fig. 5.** Particle size distribution for Si/Al<sub>2</sub>O<sub>3</sub> mixture after separation process. (a) pH=2.5; (b) pH=9.

When the cathode was installed at the inlet of the separation cell and the anode at the outlet, Si and SiC particles drifted horizontally, following the applied electrical field. However, Al<sub>2</sub>O<sub>3</sub> could not migrate easily in the applied electrical field and might settle directly near the inlet.

In addition to the surface charges, the original sizes and densities of Si, SiC and Al<sub>2</sub>O<sub>3</sub> particles are different. When a horizontal electrical field was applied to the separation system, the perpendicular gravitational force ( $F_G$ ) and horizontal electrical force ( $F_E$ ) acted on the particle and changed its motion over time. Additionally, drag force ( $F_D$ ) and buoyant force ( $F_B$ ) were also exerted on the particle, producing a complex movement path. Fig. 2 presents a schematic of this system, in which particles moved along an inclined path with an angle ( $\theta$ ) and hit the cell bottom after a period of time ( $t$ ). If the transient movement is neglected relative to the terminal state, then the horizontal displacement ( $d$ ) can be determined when Si, SiC and Al<sub>2</sub>O<sub>3</sub> particles reached the cell bottom. The relative

calculation was reported previously [12]. Table 1 presents the data and calculation results. The Si particles moved significantly farther from the inlet than the abrasives (SiC or Al<sub>2</sub>O<sub>3</sub>) because the surface charges of Si was greater than that of SiC or Al<sub>2</sub>O<sub>3</sub>. Consequently, Si can be separated from Si/SiC or Si/Al<sub>2</sub>O<sub>3</sub> theoretically. Thus, Si particles can be collected near the anode bottom and the abrasives can be collected near the cathode bottom. In addition, the separation performance of Si/Al<sub>2</sub>O<sub>3</sub> mixture might be better than that of Si/SiC mixture due to the larger difference in density and isoelectric point between Si and Al<sub>2</sub>O<sub>3</sub> than Si and SiC.

Fig. 3 shows the PSDs of original Si/SiC and Si/Al<sub>2</sub>O<sub>3</sub> mixtures in deionized water. The distributions peaked at roughly 1.6  $\mu$ m and 26  $\mu$ m for Si/SiC mixture (Fig. 3(a)), and 1.8  $\mu$ m, 18  $\mu$ m and 90  $\mu$ m for Si/Al<sub>2</sub>O<sub>3</sub> mixture (Fig. 3(b)). The size around 1  $\mu$ m was Si particles, and the size around 26  $\mu$ m and 18  $\mu$ m should be SiC and Al<sub>2</sub>O<sub>3</sub>, respectively. The size of 90  $\mu$ m in Fig. 3(b) was resulted from the agglomeration of Si and Al<sub>2</sub>O<sub>3</sub>. Because the zeta potentials of Si

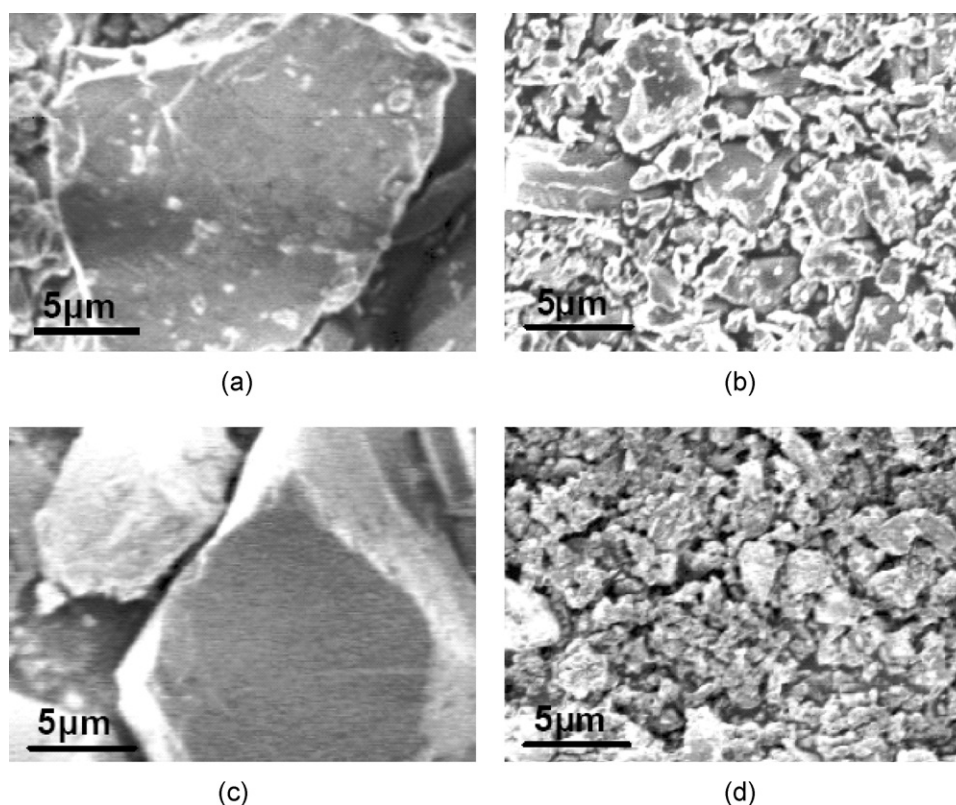


**Fig. 6.** SEM images of the samples after applying 1 V/cm for 24 h in the solution of pH 9. (a) Si/SiC at position 2; (b) Si/SiC at position 8; (c) Si/Al<sub>2</sub>O<sub>3</sub> at position 2; (d) Si/Al<sub>2</sub>O<sub>3</sub> at position 8.

and Al<sub>2</sub>O<sub>3</sub> in deionized water (pH 6.2) were  $-38$  mV and  $23$  mV, respectively (Fig. 1), Si and Al<sub>2</sub>O<sub>3</sub> particles agglomerated easily due to electrostatic attraction.

After the separation process, the particles that settled at various positions on the cell bottom were collected. The PSDs at positions 2, 5 and 8 were chosen for comparisons. Fig. 4 shows the PSDs of Si/SiC mixtures at positions 2, 5 and 8 after applying 1 V/cm for 24 h. In the pH 2.5 solution, the distributions of SiC peaked mainly at roughly  $27.21$   $\mu\text{m}$ ,  $20.07$   $\mu\text{m}$  and  $16.22$   $\mu\text{m}$  for positions 2, 5 and 8, respectively. Furthermore, an obvious Si peak ( $1.76$   $\mu\text{m}$ ) only existed at position 8 (Fig. 4(a)). The distribution indicates that the large particles settled rapidly due to an increased gravitational effect, and the small particles drifted horizontally far from the inlet. Consequently, the horizontal displacement of SiC particles was on average less than that of Si particles, meaning that SiC particles can be collected near the cathode at the cell inlet, and Si particles can be collected near the anode. However, Si and SiC particles were with few charges at pH 2.5, and would agglomerate, resulting in the SiC peak at the size larger than its original size ( $10$ – $15$   $\mu\text{m}$ ).

When the solution pH was increased to pH = 9, the Si and SiC particles carrying more negative charges repelled each other. Therefore, the distributions of SiC and Si were close to their original size and peaked at around  $11.66$   $\mu\text{m}$  and  $1.01$   $\mu\text{m}$ , respectively, as shown in Fig. 4(b). In addition, the frequency percentage of small particles for position 5 at pH 9 was higher than that at pH 2.5, showing the electrostatic driving force enhanced the Si particles to move toward the anode at pH 9.

Fig. 5 shows the PSDs of Si/Al<sub>2</sub>O<sub>3</sub> mixture after applying 1 V/cm for 24 h. In the pH 2.5 solution, the zeta potential of Al<sub>2</sub>O<sub>3</sub> was positive while that of Si was near isoelectric point, suggesting that Al<sub>2</sub>O<sub>3</sub> particles were positively charged and Si particles were neutrally charged (Fig. 1). Fig. 5(a) shows the distributions of large particles (Al<sub>2</sub>O<sub>3</sub>) peaked at roughly  $30.08$   $\mu\text{m}$  and  $18.66$   $\mu\text{m}$  at positions

2 and 5, respectively, after separation process. The main peak of Al<sub>2</sub>O<sub>3</sub> larger than its original size was due to the agglomeration of positively charged Al<sub>2</sub>O<sub>3</sub> and neutrally charged Si. Moreover, no particles  $> 10$   $\mu\text{m}$  appeared at position 8, and two obvious Si peaks ( $1.08$   $\mu\text{m}$  and  $4.46$   $\mu\text{m}$ ) existed at position 8 (Fig. 5(a)). In comparison with the PSD of Si/SiC mixture in Fig. 4(a), the frequency percentage of Al<sub>2</sub>O<sub>3</sub> peak at position 2 are greater than that of SiC, showing the positively charged Al<sub>2</sub>O<sub>3</sub> moved forward the cathode at pH 2.5. In addition, the Si particles with few charges migrated difficultly in an electrical field, but they also could disperse due to Brownian motion before hitting the cell bottom. Therefore, the small Si particles could be collected at position 8 near cell outlet. However, few charges on these Si particles readily caused the agglomeration. Thus, the settling of Si spread a wide range and peaked at more than one size.

When the solution pH was adjusted to pH = 9, the zeta potential of Al<sub>2</sub>O<sub>3</sub> was near isoelectric point while that of Si was negative, suggesting that Al<sub>2</sub>O<sub>3</sub> particles were neutrally charged, and Si particles were negatively charged (Fig. 1). After the separation, the distributions of large particles peaked mainly at roughly  $85.06$   $\mu\text{m}$  and  $24.28$   $\mu\text{m}$  at positions 2 and 5, respectively, as shown in Fig. 5(b). These peaks resulted from Al<sub>2</sub>O<sub>3</sub> but were much larger than its original size due to the agglomeration of neutrally charged Al<sub>2</sub>O<sub>3</sub> particles. Furthermore, obvious Si peaks appeared at roughly  $1$ – $2$   $\mu\text{m}$  at positions 5 and 8, showing the electrostatic driving force assisted negatively charged Si particles to move toward the anode at pH 9. At positions 8, only particles smaller than  $10$   $\mu\text{m}$  could be obtained, and the separation performance at pH 9 seemed to be better than that at pH 2.5.

Fig. 6 shows SEM images of dried Si/SiC and Si/Al<sub>2</sub>O<sub>3</sub> mixtures at positions 2 and 8 after separation process in the solution of pH 9. The large SiC or Al<sub>2</sub>O<sub>3</sub> particles could be collected at position 2 near the inlet, while the small Si particles settled with long horizontal

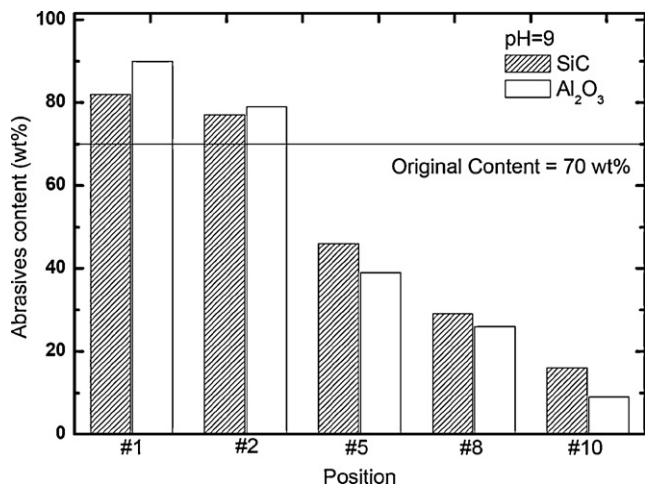


Fig. 7. Distributions of SiC and Al<sub>2</sub>O<sub>3</sub> weight percentage at different positions.

displacement. More Si particles could be collected at position 8 than position 2. At position 8, the coarse particles in Si/SiC mixture were more than in Si/Al<sub>2</sub>O<sub>3</sub> mixture. This result could be ascribed to the fact that parts of small SiC particles carrying negative charges at pH 9 moved toward the anode, and thus the separation performance for Si/Al<sub>2</sub>O<sub>3</sub> mixture could be better than that for Si/SiC.

In order to verify the separation performance for Si/SiC and Si/Al<sub>2</sub>O<sub>3</sub> mixtures, the settled particles at positions 1–10 were collected, followed by cleaning and drying. The dried Si/SiC mixtures were then analyzed by a carbon/sulfur analyzer, and the carbon content was converted to a weight percentage of SiC in the mixture. Moreover, Al<sub>2</sub>O<sub>3</sub> content in Si/Al<sub>2</sub>O<sub>3</sub> was verified using X-ray fluorescence spectrometer. Fig. 7 shows the measurement results at various positions after separation at pH = 9, where position 1 was near the inlet and position 10 near the outlet. The content of abrasives (SiC or Al<sub>2</sub>O<sub>3</sub>) decreased with the distance from inlet and was lower than the original value at positions 5–10. This experimental result is consistent with the analysis of the PSD, *i.e.* the large collected particles contained a large amount of SiC or Al<sub>2</sub>O<sub>3</sub> particles. In addition, the lower abrasives content could be found near the cell outlet for Si/Al<sub>2</sub>O<sub>3</sub> mixture than for Si/SiC mixture. The separation at position 10 was remarkable, and SiC and Al<sub>2</sub>O<sub>3</sub> content decreased to 16 wt% and 9 wt%, respectively. Furthermore, the Al<sub>2</sub>O<sub>3</sub> content in Si/Al<sub>2</sub>O<sub>3</sub> mixture was higher at positions 1 and 2 than SiC content in Si/SiC mixture, showing that using Al<sub>2</sub>O<sub>3</sub> as abrasives instead of SiC might be helpful to recycle Si and abrasives. The Si recovered near the outlet can be used in the production of solar-grade Si by a sequential high-temperature treatment and a dimensional solidification [9]. On the other hand, the abrasives collected can be reused in the sawing process.

#### 4. Conclusions

This study investigated the separation of Si/SiC and Si/Al<sub>2</sub>O<sub>3</sub> mixtures by using electrophoresis and gravitational settling. At the

isoelectric point of Si (pH = 2.5), Si and SiC particles both carried few charges, while Al<sub>2</sub>O<sub>3</sub> particles were positively charged in the mixture. As a result, the agglomeration of Si and SiC was obvious. Although the large and heavy Al<sub>2</sub>O<sub>3</sub> settled quickly, the Si particles could also be attracted to Al<sub>2</sub>O<sub>3</sub> easily. Therefore, after the application of 1 V/cm for 24 h, the separation between Si and abrasives was not good at pH 2.5. In the solution of pH 9, the Si and SiC particles, carrying more negative charges, repelled each other, while Al<sub>2</sub>O<sub>3</sub> particles were neutrally charged. The electrostatic driving force could enhance the Si particles to move toward the anode. However, Al<sub>2</sub>O<sub>3</sub> particles settled more quickly than SiC particles. Parts of small SiC particles would also move toward the anode to interfere with the Si recovery. Thus, the separation performance for Si/Al<sub>2</sub>O<sub>3</sub> mixture at pH 9 was better than that for Si/SiC. In other words, Al<sub>2</sub>O<sub>3</sub> might be a good candidate of sawing abrasives from the view of recycling Si and abrasives. However, Al is a p-type dopant and the tolerance of Al is less than 1 ppma for solar cell applications. When Al<sub>2</sub>O<sub>3</sub> is used as the abrasives for sawing silicon, the contamination of Al in the recycled silicon should be taken into consideration.

#### Acknowledgements

The author would like to thank the National Science Council of Taiwan for financially supporting this research under Contract No. NSC 99-2221-E-027-099-MY2, and thank Sino-American Silicon Products, Inc. for material assistance.

#### References

- [1] D. Sarti, R. Einhaus, Silicon feedstock for the multi-crystalline photovoltaic industry, *Sol. Energy Mater. Sol. Cells* 72 (2002) 27–40.
- [2] R.L. Billiet, H.T. Nguyen, Photovoltaic cells from silicon kerf, U.S. Patent 6,780,665, 2004.
- [3] G. Gaudet, S. Grumbine, N. Naguib, F. Batllo, Wire saw slurry recycling process, U.S. Patent 2009/0293369 A1, December 3, 2009.
- [4] A. Muller, P.M. Nasch, RE-Si-CLE: recycling of silicon rejects from PV production cycle, in: *Proc. Photovoltaic Programme, Summary Report*, Swiss Federal Office of Energy, 2004.
- [5] A. Mühlbauer, V. Diers, A. Walther, J.G. Grabmaier, Removal of C/SiC from liquid silicon by directional solidification, *J. Cryst. Growth* 108 (1991) 41–52.
- [6] S. Nishijima, Y. Izumi, S.I. Takeda, H. Suemoto, A. Nakahira, S.I. Horie, Recycling of abrasives from wasted slurry by superconducting magnetic separation, *IEEE Trans. Appl. Supercond.* 13 (2003) 1596–1599.
- [7] J. Shibata, N. Murayama, K. Nagae, Flotation separation of SiC from wastes in the silicon wafer slicing process, *Kagaku Kogaku Ronbun.* 32 (2006) 93–98.
- [8] L. Zhang, A. Ciftja, Recycling of solar cell silicon scraps through filtration, part I: experimental investigation, *Sol. Energy Mater. Sol. Cells* 92 (2008) 1450–1461.
- [9] T.Y. Wang, Y.C. Lin, C.Y. Tai, R. Sivakumar, D.K. Rai, C.W. Lan, A novel approach for recycling of kerf loss silicon from cutting slurry waste for solar cell applications, *J. Cryst. Growth* 310 (2008) 3403–3406.
- [10] T.Y. Wang, Y.C. Lin, C.Y. Tai, C.C. Fei, M.Y. Tseng, C.W. Lan, Recovery of silicon from kerf loss slurry waste for photovoltaic applications, *Prog. Photovolt.: Res. Appl.* 17 (2009) 155–163.
- [11] Y.C. Lin, T.Y. Wang, C.W. Lan, C.Y. Tai, Recovery of silicon powder from kerf loss slurry by centrifugation, *Powder Technol.* 200 (2010) 216–223.
- [12] Y.F. Wu, Y.M. Chen, Separation of silicon and silicon carbide using an electrical field, *Sep. Purif. Technol.* 68 (2009) 70–74.
- [13] D.R. Lide, *CRC Handbook of Chemistry and Physics*, 87th ed., Taylor & Francis, Florida, 2006.